

***Renilla* Luciferase Variants with Green-Peaked Emission Spectra for Improved Imaging in Living Subjects**

Andreas Markus Loening^{2,3}, Anna M. Wu¹, and Sanjiv Sam Gambhir^{1,2,3}

¹The Crump Institute for Molecular Imaging
Department of Molecular and Medical Pharmacology
Geffen School of Medicine at UCLA, Los Angeles, California
and

²Molecular Imaging Program at Stanford, Department of Radiology and Bio-X Program
Stanford University, Stanford, California
and

³Department of Bioengineering
Stanford University, Stanford, California

Running title: Red-shifted *Renilla* Luciferases

Please address all correspondence to:

Sanjiv Sam Gambhir, M.D., Ph.D.
Stanford University School of Medicine
Department of Radiology and Bio-X Program
The James H. Clark Center
318 Campus Drive, Clark E150
Stanford, CA 94305-5427
Phone: 650-725-2309
FAX: 650-897-9988
sgambhir@stanford.edu

Abstract

Renilla luciferase (RLuc) is commonly used as a reporter gene either on its own, or in conjunction with firefly and other beetle luciferases. Its use in small animal imaging, however, has been hampered by its 481 nm peaked emission spectrum as blue wavelengths are strongly attenuated in biological tissues. To overcome this difficulty, we focused on red-shifting RLuc through a combination of semi-rational and random mutagenesis yielding variants with bathochromic shifts of up to 66 nm (547 nm peak). Analysis of the most promising variant demonstrated it was 6-fold brighter than RLuc, and its green emission spectrum (535 nm peak) generated a further ~3-fold improvement in photon transport at depths of 1-2 mm of animal tissue. This is a significant improvement for bioluminescence imaging over previous RLuc variants, and should greatly aid the use of *Renilla* luciferase as an *in vivo* reporter gene.

Introduction

Luciferases are commonly employed as reporter genes in a variety of biological assays performed in the context of both cell culture as well as small animal disease models. When measuring cell culture samples for luciferase activity, the wavelength of light that the luciferase yields is usually of little consequence. In contrast, for imaging in intact animals it is highly advantageous for a luciferase to emit a large percentage of its photons in the red to near-infrared wavelengths (600-900 nm), as tissue attenuation of optical wavelength photons is minimized in this region of the spectrum [1].

For small animal imaging applications, the luciferases utilizing D-luciferin as their substrate (e.g. firefly, click beetle red) have been the preferred enzymes, as their emission peaks (540-615 nm) result in an appreciable fraction of the emitted photons to be of wavelengths greater than 600 nm. In both cell culture and animal experiments, the luciferases utilizing coelenterazine as their substrate (e.g. *Renilla*, *Gaussia*) have served as useful adjuncts to the beetle luciferases [2, 3]. They have also seen employment in situations where the ATP-dependence and poor thermal stability of the beetle luciferases would be a liability, such as in bioluminescently tagged imaging probes [4] and self-illuminating quantum dots [5]. The coelenterazine luciferases, however, suffer the major limitation when it comes to most small animal imaging applications that their spectral peaks lie in the blue region of the visible spectrum. In the case of *Renilla* luciferase (RLuc), the spectral peak lies at 481 nm, and only $\sim 3\%$ of the emitted photons are of wavelengths above 600 nm. As pointed out later in the text, for luciferase locations at anything deeper than subcutaneous depths, the majority of the photons that actually make it out of the animal are these few >600 nm wavelength photons [6]. Clearly, a *Renilla* luciferase with a bathochromic (red) shifted emission spectrum, and therefore a greater number of >600 nm wavelength photons, would be advantageous for use in small animal imaging.

The theory behind shifting the bioluminescence emission spectrum of RLuc starts with an understanding of the luminescence reaction. As shown in Figure 1a, the reaction starts with coelenterazine and molecular oxygen, and yields carbon dioxide, coelenteramide, and a photon of light. The reaction goes through a dioxetane (also called dioxetanone or cyclic peroxide) intermediate step [7], and the break down of this high-energy bond leaves an electron in the resultant coelenteramide in an excited electronic state. At this point, the electron/coelenteramide system can lose energy and return to the ground electronic state through a number of processes, with the desired transition in bioluminescence being the conversion of the energy into a photon of light. The emitted

photon's wavelength will depend directly on the energy difference between the excited and ground states, which in turn will depend on the local chemical environment in which the coelenteramide finds itself.

The chemical state that the excited-state coelenteramide is in within the bioluminescence reaction can be investigated by exposing coelenteramide to a variety of solvents, so as to achieve different anions of the compound, measuring its fluorescence, and then correlating the fluorescence spectrum to the spectrum that is observed as a product of bioluminescence. Through such work, it has been suggested that the blue light emission (481 nm peak for RLuc) associated with coelenterazine bioluminescence is due to the excited state coelenteramide existing in its amide anion form (Figure 1b) when it is in the protein's enzymatic pocket [8]. For RLuc, the literature has historically agreed with this assignment of the emitting species [9, 10]. However, at least in the case of photoproteins that utilize coelenterazine such as obelin and aequorin, more recent literature has favored assigning the phenolate anion as the blue emitting species in bioluminescence [11, 12, 13].

An interesting observation from this previous work, is that coelenteramide can be shown to emit a green fluorescence (535-550 nm) when it is in particular chemical environments. Recognition that coelenteramide can achieve an anionic state in which it fluoresces green led to the hypothesis that, by proper alteration of the enzymatic pocket of the luciferase, the necessary chemical environment could be attained within RLuc so as to favor the green emitting anion form. If the blue light emitter in RLuc bioluminescence is indeed the phenolate anion and the green fluorescent form is the pyrazine anion, one can imagine that favoring the pyrazine anion resonance form of the coelenteramide molecule will lead to a bathochromic shift in the emission spectrum.

We hypothesized that appropriate alteration of RLuc's enzymatic pocket could alter the chemical environment coelenteramide experiences and in turn favor a product species that would emit a green photon of light. For practical reasons, we focused on modifying a previously described 8-mutation variant of RLuc, called RLuc8, that is both more stable and emits more light than the native enzyme [14]. This work begins with predictions regarding the active pocket of RLuc8, followed by site specific mutagenesis studies of the predicted catalytic pocket residues in an attempt to red-shift the emission spectrum of the protein. Additional iterations of random mutagenesis were then done in a successful attempt to generate viable, >50-60 nm red-shifted variants of *Renilla* luciferase. Finally, the applicability of these variants was demonstrated in both cell culture and small animal imaging experiments.

Results

Homology Model/Putative Active Site

In an attempt to rationally alter the emitted wavelength of *Renilla* luciferase, the location and orientation of the substrate in the active pocket was conjectured within a homology model of RLuc8 (Figure 1c). This was done by assuming the catalytic triad of D120/E144/H285 identified previously [14] was used for coordinating the oxygen, that the orientation of the substrate would be similar to that seen with other similar α/β -hydrolase fold proteins [15], and that the varying affinities of various mutations for several coelenterazine analogs [14] was due to close interactions between the mutation and the altered side chain of the analog. The results of this exercise indicated which residues were likely to interact with the substrate and are shown in Figure 1d. These putative active pocket amino acids are marked in the primary sequence shown in Supplemental Figure 1.

Mutagenesis Probing of the Active Site of RLuc8

Using this model of coelenterazine/coelenteramide in the active pocket as a guide, a total of 74 site specific mutations were made at the 22 residues thought to interact with the substrate. With the exception of the I223 location at which mutagenesis was saturating, the subset of possible mutations done at each residue was selected based on what would be considered “safe” with respect to the tertiary fold of the enzyme [16]. The pertinent results of this screen are presented in Table 1 (Full data in supplemental Tables 1 and 2), with several of the resultant color shifts visually displayed in Figure 2a. From this screen, a total of 21 mutations at 10 different residue locations resulted in observable shifts in the emission spectrum. The variants with bathochromic shift mutations presumably have active pockets that favor the green fluorescing anion form of coelenteramide. Unsurprisingly, given that the enzymatic pocket of *Renilla* luciferase is already evolved for the reaction at hand, nearly all these mutations led to significant reductions in the light output of the luciferase.

Random Mutagenesis on RLuc8

At this point, a random mutagenesis study was undertaken in the hopes of recovering the catalytic abilities of some of the above red-shifted variants as well as to probe for variants with further

red-shifts in their emission spectra. The RLuc8/F261W and RLuc8/F262W variants were picked as starting points, as they both gave rise to appreciable bathochromic shifts while not overly compromising the light output of the luciferase. Random mutagenesis was performed on these templates, and screened in bacteria for both increases in light output as well as emission color shifts (results in Supplemental Table 3). Interestingly, several mutation locations were overrepresented. Of these mutations, those at residues E155 and G269 lead to increases in light output, and those at D162 resulted in further bathochromic shifts in the emission spectra.

Based on the site-specific and random mutagenesis results, several serial rounds of site-specific random mutagenesis were performed. The templates RLuc8, RLuc8/A123S, RLuc8/A123S/F261W, and RLuc8/A123S/F262W were used initially, with successfully improved constructs incorporated as the starting templates for later rounds. As inclusion of a neighboring residue in addition to the target residue could easily be incorporated within the scale of each experiment, two adjacent amino acids were mutated in each step. In some cases, the choice of the additional residue was made on rational grounds. For instance, the D162 residue identified in the random mutagenesis screen borders the putative active pocket residue I163, so this residue was selected for inclusion in the site-directed random mutagenesis screen.

The initial round of mutagenesis was done at D162/I163, followed by rounds at F261/F262, I223/P224, V185/I186, D154/E155, and G269/A270. The most promising results from these screens are presented in Table 1, with the visual appearance and measured spectra of these variants when combined with coelenterazine shown in Figure 2. Additional emission data for these variants with several analogs of coelenterazine is given in Supplemental Table 7. More complete results of the D162/I163, V185/I186, and D154/E155 screens are given in Supplemental Tables 4, 5, and 6, respectively. Results of mutagenesis screens at locations F261/F262, I223/P224, as well as G269/A270 did not lead to improved constructs and the results are not reported.

In an attempt to identify locations that might yield further red-shifts in the bioluminescence emission spectrum, the RLuc8.6-547 construct (Table 1) was subjected to random mutagenesis. In a small screen of ~15,000 colonies, no further improvements in either light output or emission spectrum red-shifts were observed.

Evaluation in Cell Culture

To demonstrate the applicability of the generated RLuc variants as mammalian reporter genes, expression vectors were constructed for RLuc, RLuc8, and RLuc8.6-535 in a pcDNA 3.1 back-

bone. These plasmids were studied in transfection experiments utilizing 293T cells. The results, shown in Figure 3a, indicate that when used as a reporter gene RLuc8.6-535 exhibits significantly greater signal than RLuc and RLuc8, and has a similar intracellular half-life to RLuc8.

Evaluation in Small Animal Imaging

To evaluate the gain that a red-shifted emission spectrum would display in the context of animal tissue, purified RLuc8.6-535 protein was injected into the thigh musculature of mice (depth of ~1-2 mm), with the contralateral thigh injected with RLuc8 as a control. The results, presented in Figures 3c, 3d, and 3e, show that for an equivalent level of *ex vivo* activity RLuc8.6-535 allows transmission of 2.6-fold more light than RLuc8 following intramuscular injection of protein.

To further test the gain of the red-shifted emission spectra, cells transiently transfected with either RLuc8 or RLuc8.6 were injected into the tail vein of mice. Cells injected in this manner are initially trapped predominately in the lung, and as shown in Figure 3b the red-shifted emission spectra of RLuc8.6 yields a 2.2-fold increase in signal from the lungs of these animals.

Discussion

It was unclear before starting this work whether a protein could present the necessary chemical environment to favor the green emitting anion form of coelenteramide (presumably the pyrazine anion, Figure 1b). The main evidence against being able to achieve this anionic form in the context of a protein is that no known coelenterazine using bioluminescent proteins are able to directly emit a green-peaked emission spectrum. There are cases where green bioluminescence is observed from organisms with known coelenterazine using luciferases or photoproteins (e. g. *Renilla reniformis*, *Aequorea victoria*), but the green light emission in these cases has always been found to be due to bioluminescence resonance energy transfer (BRET) from a blue emitting luciferase or photoprotein to a green fluorescent protein (GFP). If a green emission spectrum from a coelenterazine using luciferase was possible, why would the more complex solution of having an accessory fluorescent protein have evolved?

The data presented here shows that a green emitting coelenterazine using luciferase is indeed possible, presumably due to favoring the pyrazine anion of coelenteramide in the enzymatic pocket. Further more, this shift in spectrum can come without loss in the ability of the luciferase to emit

light. So why then have many marine organisms evolved to exhibit a luciferase/GFP BRET pair? One hypothesis arises from a comparison of the GFP and green emitting luciferase spectra (shown in Supplemental Figure 2). Such a comparison highlights the broad emission spectra of the luciferases and the relatively narrow emission of the GFP. Presumably, there is an evolutionarily advantageous reason for *Renilla reniformis* to emit green light, and the use of a GFP allows a greater number of the emitted photons to be at these desired wavelengths.

Quite surprisingly, a single point mutation (D162E) was found that could lead to a large red-shift of the emission spectra of the luciferase without a severe compromise in the luciferase's ability to output light. This single mutation was responsible for ~60% of the total bathochromic shift that we were able to achieve through the course of this study. Another surprising finding, was that several of the mutants had side peaks around 410 nm. This side peak is presumptively emanating from the neutral species of coelenteramide. Although not explored here, it would be intriguing to see if appropriate mutagenesis of *Renilla* luciferase could lead to a variant with a pure violet (410 nm) emission peak.

An interesting question to ask, is how much of an effect on *in vivo* imaging capabilities could one expect from the ~25-65 nm emission shifts of the luciferase variants presented here, especially given that these bathochromic (red) shifts move the emission peak into a local maximum around 550 nm in the hemoglobin absorption curve. To answer this question, rough calculations of light attenuation were made by multiplying rat liver transmittance values [17, 18] by the normalized emission spectra for several of the luciferases, including those from the click beetle (Figure 2b). These calculated transmitted emission spectra are shown in Supplemental Figure 3. At 1 mm of tissue depth, the main spectral peak of *Renilla* luciferase is severely diminished, and at 5 mm depth one can observe that it is really only the photons with wavelengths >600 nm that are able to escape from the tissue, underscoring the importance of these few long wavelength photons in allowing the detection of this luciferase in small animal imaging. Other highlights from this comparison are that for an equal number of generated photons the green emitting RLuc variants should perform as well as click beetle green *in vivo*, and that the emission spectra from all these luciferases are essentially identical in form after filtering through biological tissue.

A quantitative comparison is given in Table 2, where predictions are made as to the relative gain in light output versus RLuc for the various luciferase variants at 1 and 5 mm depth of liver tissue. Again, these results underscore the advantageousness of having a red-shifted *Renilla* luciferase for small animal imaging applications. They also point out that the benefits of red-shifting the emission spectrum outweigh any penalties from the local hemoglobin absorption peak at 550 nm.

Although muscle tissue was used as the absorber for the *in vivo* experiments shown in Figure 3e, the 2.6-fold gain for RLuc8.6-535 versus RLuc8 for 1-2 mm of thigh muscle tissue corresponds well with the ~ 3 -fold gain predicted here for 1 mm of liver tissue.

In an experiment in which transiently transfected cells were injected intravenously into mice (Figure 3b), imaging of these cells lodged in the lungs demonstrated that the green-peaked emission spectrum of RLuc8.6-535 resulted in a ~ 2 -fold increase in light penetration through the chest wall. Note that, as half the number of RLuc8.6-535 as RLuc8 transfected cells were injected, RLuc8.6-535 actually led to a signal gain of 4.4-fold on a per cell basis in comparison to RLuc8. In turn, it can be estimated that RLuc8.6-535 would yield ~ 40 -fold more signal per cell in this experimental context than RLuc, based on the cell culture (Figure 3a) and animal results.

BRET methodologies, utilizing RLuc as the donor, have recently been applied for non-invasively measuring protein-protein interactions within small animals [19]. To use BRET to its full effectiveness, both donor and acceptor signals need to be recorded. This has been problematic in the *in vivo* situation, due to the preferential tissue attenuation of the shorter wavelength donor signal. Work is currently ongoing in our laboratory to examine the possibility of combining the green-emitting RLuc variants developed here with appropriate red-shifted fluorescent proteins [20] in order to generate BRET systems more appropriate for use in small animals.

An interesting observation for cell culture BRET work, is that the various RLuc variants developed here maintain the ~ 400 nm wavelength peak that is seen with the native luciferase in the presence of bisdeoxycoelenterazine (Supplemental Table 7). This raises the intriguing possibility that the interaction of a protein with two separate partners could be assessed simultaneously. For instance, RLuc8.6-535 could be fused to a protein of interest as the BRET donor, and two interacting partners could be fused to either EBFP or mOrange as the acceptor moiety. Following the simultaneous application of coelenterazine and bisdeoxycoelenterazine, both 400 nm and 535 nm donor light would result, and depending on the interacting partner present, either 445 nm or 560 nm BRET light would be emitted as well.

Two proprietary analogs of coelenterazine, EnduRen and ViviRen, have recently been brought to market by Promega, with ViviRen showing promise for increasing the signal obtained in small animal imaging studies utilizing *Renilla* luciferase [21]. Both of these molecules are pro-substrates, and are transformed into the active substrate benzyl-coelenterazine by intracellular esterases. Testing of the *Renilla* variants developed here with benzyl-coelenterazine showed similar results to that which was obtained with native substrate (Supplemental Table 7), indicating there are no limitations to applying the variants in experiments utilizing these novel coelenterazine analogs.

The work presented here describes *Renilla* luciferase variants with green-peaked emission spectra. As even further red-shifts in the emission spectrum would be desirable for the purposes of *in vivo* imaging, the question becomes can further red-shifts be achieved? As the amount of interaction between the luciferase and the luciferin is not well understood a conclusive answer cannot be stated at this time, but it may be that the pyrazine anion of coelenteramide represents a limit as to the bathochromic shift that this luciferin/luciferase system can accomplish. As further bathochromic shifts of the emission spectrum may not be achievable from mutagenesis of the luciferase, it may be more fruitful at this point to consider altering the structure of the luciferin. Analogs of coelenterazine that emit longer wavelengths of light when catalyzed by *Renilla* luciferase have been synthesized [22, 23, 24]. The most promising analog, coelenterazine-*v*, has been shown to exhibit a high level of bioluminescence with RLuc while yielding an ~ 35 nm red shifted emission compared to the native substrate. Hopefully, the combination of such a red-shifted coelenterazine analog and a luciferase variant capable of placing the analog in its pyrazine anion state will result in an additive effect leading to an orange emission spectra.

Methods

Materials

Coelenterazine was obtained from Prolume (Pinetop, AZ), dissolved in propylene glycol, and stored in small aliquots at -80°C .

Luminometer Calibration

Light measurements were made using a Turner 20/20n luminometer (Turner Designs, Sunnyvale, CA). The luminometer was calibrated to absolute units (photons/s) using the luminol light standard performed in dimethyl sulfoxide (DMSO) [25, 26, 27]. Reported luminometer readings were corrected for the spectral sensitivity of the R1924P photomultiplier tube [28]. Corrections varied from 0.6 for spectra with a 400 nm mean emission to 2.0 for spectra with a 560 nm mean emission.

Computational Prediction

A homology model of RLuc8 was built with SWISS-MODEL (v3.5) [29] using the default parameters (Figure 1c). In generating this homology model, SWISS-MODEL utilized several crystal structures of the haloalkane dehalogenase LinB from *Sphingomonas paucimobilis* (PDB files 1iz8, 1k63, 1k6e, 1iz7, and 1mj5). The molecule of coelenterazine was modeled in by hand, with the location and orientation determined using the rationale described in the results section.

Construction of *Renilla* Luciferase Mutants

The plasmid pBAD-pelB-RLuc8 [14] was used as the initial starting point for all mutagenesis. This plasmid encodes a stabilized variant of RLuc, “RLuc8”, containing 8 mutations (A55T, C124A, S130A, K136R, A143M, M185V, M253L, and S287L). The pelB leader sequence, consisting of the first 22 codons of the pectate lyase B gene from *Erwinia carotovora* [30], directs protein expression into the bacterial periplasm and is cleaved from the final protein product. Site directed mutagenesis was performed using standard protocols [31, 27]. All constructs and mutations were confirmed by sequencing.

Random Mutagenesis

Random mutagenesis was accomplished using Mutazyme II (Stratagene, La Jolla, CA) following the manufacturer’s protocol, with the alteration of 5% DMSO added to the reaction mixture. A template concentration of 15 pg pBAD-pelB-RLuc8 plasmid in a 50 μ l reaction volume with 50 rounds of PCR was used to give a mutation rate of \sim 5 base pairs/kb. The primers contained appropriate restriction sites (NcoI/SalI) to allow reinsertion into the plasmid backbone. Ligated product was transformed into Top10 bacterial cells (Invitrogen) and spread on Terrific Broth/50 μ g/ml ampicillin (TB/Amp) agar plates containing 0.2% L-(+)-arabinose. Following 20 h of incubation at 32°C, the plates were airbrushed with a phosphate buffered saline (PBS) solution containing 5 μ g/ml coelenterazine and imaged immediately using an IVIS 200 bioluminescence imaging system (Xenogen). Three 5 s acquisitions were made using a DsRed, a GFP, and an open filter. Acquired images were processed in GNU Octave [32] using a collection of custom scripts. Colonies were selected for brightness and/or spectral shifts both automatically using the above mentioned scripts as well as manually. Colonies were then screened further as described below.

Site-specific Random Mutagenesis

Random mutagenesis at specific locations was performed by making use of Type II restriction enzymes and primers containing a randomized codon sequence. The method used here was a modification of a previously published protocol [33], differing mainly in that the entire plasmid was used as the template for PCR obviating the need for a second ligation step. The protocol is schematically outlined in Supplemental Figure 4. For the PCR, the conditions used were those recommended for the Pfu Ultra polymerase by the manufacturer (Stratagene), with the exceptions that extension time was increased to 2 min/kb, 5% DMSO was included in the reaction, template was used at 10% of usual concentrations, and primers were used at 20% of usual concentrations. A restriction digest using BpiI (Fermentas, Hanover, MD), along with DpnI to remove remaining template, was performed overnight in a 37°C bacterial incubator. Following gel purification, ligation, transformation, plating, and initial screening was done as in the random mutagenesis case, with further screening proceeding as described below. Generally, 5,000-10,000 colonies were screened in each site-specific random mutagenesis experiment.

Further Screening, Protein Production and Purification

For random mutagenesis experiments, the clones initially selected from the agar plates were further screened by small scale expression experiments. Selected colonies were picked into 2 ml TB/Amp each and grown to saturating conditions at 37°C (~12 h). 2 ml TB/Amp containing 0.2% L-(+)-arabinose was then added to each tube and the cultures were grown an additional 12 h at 32°C. Following this, half of each culture was spun down and submitted to osmotic shock [34]. The periplasmic fractions were assayed for specific activity, assessed for bioluminescence color shifts visually, and stored at 4 °C. Bright and/or color shifted variants were then submitted for sequencing. For variants identified as having novel mutations, the periplasmic fraction was brought to 300 mM NaCl, 20 mM HEPES, 20 mM imidazole, pH 8 from a 10x stock, further purified using nickel affinity spin columns (Ni-NTA Spin Kit, Qiagen) with 300 mM NaCl, 20 mM HEPES, 250 mM imidazole, pH 8 as the elution buffer, and brought to 1% human serum albumin (Baxter Healthcare Corporation, Glendale, CA).

For site-specific mutagenesis experiments, protein expression was done in *E. coli* LMG 194 cells using periplasmic (pelB containing) expression plasmids as previously described [14].

Characterization of *Renilla* Luciferase Mutants

Luciferase activity and emission spectra were measured as previously described [14]. Unless otherwise specified, all activity and spectra measurements were made using coelenterazine, and all activity measurements were corrected for the luminometer's wavelength-dependent sensitivity. Emission spectra were filtered as necessary and normalized to equalize the total area under the curve.

Mammalian Expression

Mammalian expression vectors were constructed and tested in cell culture using transient transfection in 293T cells as previously described [14].

Animal Experiments

In preparation for injection into animals, purified proteins were buffer exchanged into PBS and diluted so that equivalent volumes would yield equivalent amounts of light. A volume of 10 μ l (0.11 μ g RLuc8 or 0.08 μ g RLuc8.6-535) was then injected into the thigh musculature of nu/nu mice, with the contralateral thigh receiving an injection of purified RLuc8 as the control. These animals were injected with coelenterazine and imaged immediately as described below. As an alternative model, 293T cells, transiently transfected as previously described [14], were injected into the left tail vein of nu/nu mice with the animals imaged 30 min later. The infusion was 1×10^6 cells for the RLuc8 transfected cells, and half this number for the RLuc8.6-535 condition, in order that equal numbers of photons could be expected from the two conditions. For all imaging, a solution of 10 μ g of coelenterazine in 100 μ l PBS was injected into the right tail vein, with the animal imaged immediately in an IVIS 200. Acquisition times were 10 s for the open filter, and 30 s for the other filters. All injections and imaging were done under isoflurane anesthesia, and all animal work was approved by Stanford University's Administrative Panel on Laboratory Animal Care (APLAC).

Acknowledgments

This work was supported in part by a Stanford Bio-X Graduate Fellowship (AML), NCI CA114747 ICMIC P50 (SSG), and the NCI SAIRP. The authors would like to thank Dr. Brad Rice and Dr. Tamara Troy of Xenogen Corporation for help with the spectra measurements.

Competing Financial Interests

The authors declare competing financial interests.

References

- [1] Weissleder, R. A clearer vision for *in vivo* imaging. *Nat. Biotechnol.* **19**, 316–317 (2001).
- [2] Bhaumik, S. & Gambhir, S. S. Optical imaging of *Renilla* luciferase reporter gene expression in living mice. *Proc. Natl. Acad. Sci.* **99**, 377–382 (2002).
- [3] Shah, K., Tang, Y., Breakefield, X. & Weissleder, R. Real-time imaging of trail-induced apoptosis of glioma tumors in vivo. *Oncogene* **22**, 6865–6872 (2003).
- [4] Venisnik, K. M. *et al.* Bifunctional antibody-*Renilla* luciferase fusion protein for *in vivo* optical detection of tumors. *Protein Eng. Des. Sel.* **19**, 453–460 (2006).
- [5] So, M. K., Xu, C., Loening, A. M., Gambhir, S. S. & Rao, J. Self-illuminating quantum dot conjugates for in vivo imaging. *Nat. Biotechnol.* **24**, 339–343 (2006).
- [6] Zhao, H. *et al.* Emission spectra of bioluminescent reporters and interaction with mammalian tissue determine the sensitivity of detection *in vivo*. *J. Biomed. Opt.* **10**, 41210 (2005).
- [7] Hart, R. C., Stempel, K. E., Boyer, P. D. & Cormier, M. J. Mechanism of the enzyme-catalyzed bioluminescent oxidation of coelenterate-type luciferin. *Biochem. Biophys. Res. Commun.* **81**, 980–986 (1978).
- [8] Shimomura, O. & Teranishi, K. Light-emitters involved in the luminescence of coelenterazine. *Luminescence* **15**, 51–58 (2000).

- [9] Hori, K., Wampler, J. E., Matthews, J. C. & Cormier, M. J. Identification of the product excited states during the chemiluminescent and bioluminescent oxidation of *Renilla* (sea pansy) luciferin and certain of its analogs. *Biochemistry* **12**, 4463–4468 (1973).
- [10] Matthews, J. C., Hori, K. & Cormier, M. J. Purification and properties of *Renilla reniformis* luciferase. *Biochemistry* **16**, 85–91 (1977).
- [11] Imai, Y. *et al.* Fluorescence properties of phenolate anions of coelenteramide analogues: the light-emitter structure in aequorin bioluminescence. *J. Photochem. Photobiol. A: Chem.* **146**, 95–107 (2001).
- [12] Vysotski, E. S. & Lee, J. Ca²⁺-regulated photoproteins: Structural insight into the bioluminescence mechanism. *Acc. Chem. Res.* **37**, 405–415 (2004).
- [13] Liu, Z. J. *et al.* Crystal structure of obelin after Ca²⁺-triggered bioluminescence suggests neutral coelenteramide as the primary excited state. *Proc. Natl. Acad. Sci.* **103**, 2570–2575 (2006).
- [14] Loening, A. M., Fenn, T. D., Wu, A. M. & Gambhir, S. S. Consensus guided mutagenesis of *Renilla* luciferase yields enhanced stability and light output. *Protein Eng. Des. Sel.* **19**, 391–400 (2006).
- [15] Streltsov, V. A. *et al.* Haloalkane dehalogenase LinB from *Sphingomonas paucimobilis* UT26: X-ray crystallographic studies of dehalogenation of brominated substrates. *Biochemistry* **42**, 10104–10112 (2003).
- [16] Bordo, D. & Argos, P. Suggestions for “safe” residue substitutions in site-directed mutagenesis. *J. Mol. Biol.* **217**, 721–729 (1991).
- [17] Cheong, W. F., Prahl, S. A. & Welch, A. J. A review of the optical properties of biological tissues. *IEEE J. Quantum Electron.* **26**, 2166–2185 (1990).
- [18] Cheong, W. F., Prahl, S. A., Welch, A. J., Wang, L. & Jacques, S. L. Optical properties of biological tissues. on the World Wide Web at <http://omlc.ogi.edu/pubs/abs/cheong90a.html> (1993).
- [19] De, A. & Gambhir, S. S. Noninvasive imaging of protein-protein interactions from live cells and living subjects using bioluminescence resonance energy transfer. *FASEB J.* **19**, 2017–2019 (2005).

- [20] Wang, L., Jackson, W. C., Steinbach, P. A. & Tsien, R. Y. Evolution of new nonantibody proteins via iterative somatic hypermutation. *Proc. Natl. Acad. Sci.* **101**, 16745–16749 (2004).
- [21] Otto-Duessel, M. *et al.* *In vivo* testing of *Renilla* luciferase substrate analogs in an orthotopic murine model of human glioblastoma. *Mol. Imaging* **5**, 57–64 (2006).
- [22] Shimomura, O., Musicki, B. & Kishi, Y. Semi-synthetic aequorin. an improved tool for the measurement of calcium ion concentration. *Biochem. J.* **251**, 405–410 (1988).
- [23] Inouye, S. & Shimomura, O. The use of *Renilla* luciferase, *Oplophorus* luciferase, and apoaequorin as bioluminescent reporter protein in the presence of coelenterazine analogues as substrate. *Biochem. Biophys. Res. Commun.* **233**, 349–353 (1997).
- [24] Wu, C., Nakamura, H., Murai, A. & Shimomura, O. Chemi- and bioluminescence of coelenterazine analogues with a conjugated group at the c-8 position. *Tetr. Lett.* **42**, 2997–3000 (2001).
- [25] Lee, J., Wesley, A. S., Ferguson, J. F., III & Seliger, H. H. The use of luminol as a standard of photon emission. In Johnson, F. H. & Haneda, Y. (eds.) *Bioluminescence in Progress*, 35–43 (Princeton University Press, Princeton, New Jersey, 1966).
- [26] O’Kane, D. J. & Lee, J. Absolute calibration of luminometers with low-level light standards. *Methods Enzymol.* **305**, 87–96 (2000).
- [27] Loening, A. M. *Technologies for imaging with bioluminescently labeled probes*. Ph.D. thesis, Leland Stanford Junior University (2006).
- [28] Hamamatsu Photonics K.K., Hamamatsu City, Japan. *Photomultiplier Tubes, Basics and Applications*, second edn. (1999).
- [29] Schwede, T., Kopp, J., Guex, N. & Peitsch, M. C. SWISS-MODEL: an automated protein homology-modeling server. *Nucl. Acids Res.* **31**, 3381–3385 (2003).
- [30] Lei, S. P., Lin, H. C., Wang, S. S., Callaway, J. & Wilcox, G. Characterization of the *Erwinia carotovora* pelB gene and its product pectate lyase. *J. Bacteriol.* **169**, 4379–4383 (1987).
- [31] Weiner, M. P. *et al.* Site-directed mutagenesis of double-stranded DNA by the polymerase chain reaction. *Gene* **151**, 119–123 (1994).

- [32] Eaton, J. W. *GNU Octave: A High-Level Interactive Language for Numerical Computations* (Network Theory, Clifton, UK, 1997), third edn.
- [33] Ko, J.-K. & Ma, J. A rapid and efficient PCR-based mutagenesis method applicable to cell physiology study. *Am. J. Physiol. Cell Physiol.* **288**, C1273–C1278 (2005).
- [34] Neu, H. C. & Heppel, L. A. The release of enzymes from *Escherichia coli* by osmotic shock and during the formation of spheroplasts. *J. Biol. Chem.* **240**, 3685–3692 (1965).
- [35] Deng, L. *et al.* Structural basis for the emission of violet bioluminescence from a W92F obelin mutant. *FEBS Lett.* **506**, 281–285 (2001).
- [36] Viviani, V. R., Oehlmeyer, T. L., Arnoldi, F. G. & Brochetto-Braga, M. R. A new firefly luciferase with bimodal spectrum: identification of structural determinants of spectral ph-sensitivity in firefly luciferases. *Photochem. Photobiol.* **81**, 843–848 (2005).
- [37] Holm, S. A simple sequentially rejective multiple test procedure. *Scand. J. Stat.* **6**, 65–70 (1979).

Legends to Figures

- 1 *Renilla* luciferase’s luminescence reaction, different anionic states of the product, and estimates as to the interaction of the protein with the substrate. 18
 - (a) The luminescence reaction catalyzed by *Renilla* luciferase is shown with the phenolate anion of coelenteramide as the emitting species, although assignment of the emitting species’ exact state is a matter of contention (see main text). 18
 - (b) The different potential anionic states of the reaction’s product, coelenteramide, are shown along with the the fluorescence emission peak thought to be associated with each species [8, 35]. Note that the phenolate and pyrazine anions are different resonant structures of the same molecule. 18
 - (c) The estimated orientation of the substrate, coelenterazine, is shown within the RLuc8 homology structure. The N-terminus of the structure is in blue, the C-terminus is in red, and the substrate is shown in black. In addition to the estimated substrate location, the catalytic triad of D120, E144, and H285 is shown as well. 18
 - (d) The same information shown diagrammatically. These putative active site residues thought likely to interact with coelenterazine became targets for site-directed mutagenesis. 18
- 2 Mutations of *Renilla* luciferase led to appreciable shifts in the emission spectrum. . 19
 - (a) Color photographs for several of the variants developed in this paper. The images shown were made by mixing purified protein with coelenterazine, and photographing the resultant emission with a consumer-grade digital camera. 19
 - (b) Normalized bioluminescence emission spectra for several of the RLuc variants as well as the click beetle luciferases. The spectra for the click beetle luciferases, included for comparison, are from Zhao *et al.* [6] and were measured using D-luciferin. Note that the emission spectrum of firefly luciferase is variable, depending upon both temperature and its chemical environment [36], and would lie somewhere intermediate to the spectra for click beetle green luciferase and click beetle red luciferase. Normalization was to the total area under the curve, and not the emission peak. 19
- 3 Testing of RLuc8.6-535 in cell culture along with animal model experiments demonstrating the effects of emission spectra on the transmission of *Renilla* luciferase bioluminescence through tissue. 20

- (a) Mammalian cell expression of native RLuc, RLuc8, and RLuc8.6-535 following transient transfection into 293T cells. The luciferases were in pcDNA 3.1 plasmids under the control of the constitutive promoter from cytomegalovirus (CMV). Cycloheximide (100 μ g/ml final) was applied 48 hrs following transfection. Light output per total cellular protein is reported as relative to the value of the RLuc condition prior to application of cycloheximide. All differences between groups for a given time point were significant at $p \leq 0.01$ using a two-tailed t -test with the incorporation of a Bonferroni-Holms correction for multiple comparisons [37]. Estimated half-lives are given in parenthesis in the figure key. Samples were in quadruplicate, and error bars represent standard error of the mean. 20
- (b) Mean emission fluxes from ROIs drawn over the lungs of mice injected with 293T cells transfected with RLuc8 or RLuc8.6-535. For RLuc8.6-535, half the number of cells were injected so that the initial light flux in each group would be equal. Five animals were used per group, and the abdomen was used as the background measurement. Differences were significant at $p < 0.05$ using a one-tail Student t -test, and error bars represent standard error of the mean. 20
- (c) A representative animal scan from nine nu/nu mice injected with RLuc8.6-535 in the thigh with an equivalent activity of RLuc8 injected in the contralateral thigh. Imaging was performed using open, 480 nm, 540 nm, and 600 nm filters. The tissue depth of the injection sites was estimated to be between 1-2 mm. The open filter images are displayed with a max/min scale of $1 \times 10^7/4 \times 10^4$ photons/s/cm²/steradian. The other filters are displayed with a max/min scale of $4 \times 10^5/2 \times 10^4$ photons/s/cm²/steradian. 20
- (d) Total emission fluxes from regions of interest (ROIs) drawn over the thighs in question, with the left arm used as background. Total flux from the ROI was used as the measurement, and plots are drawn with error bars representing standard error of the mean. Differences between the open, 480 nm, and 600 nm filter images were significant at $p < 0.01$ using paired two-tailed Student t -tests. 20
- (e) The ratio of the emission flux from the thigh containing RLuc8.6-535 over that from the thigh containing RLuc8. 20

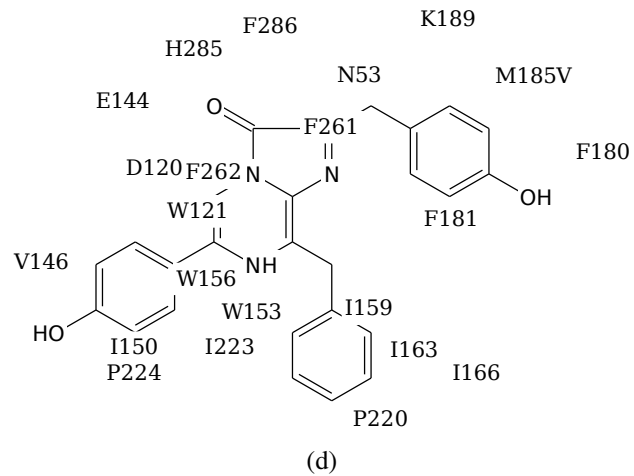
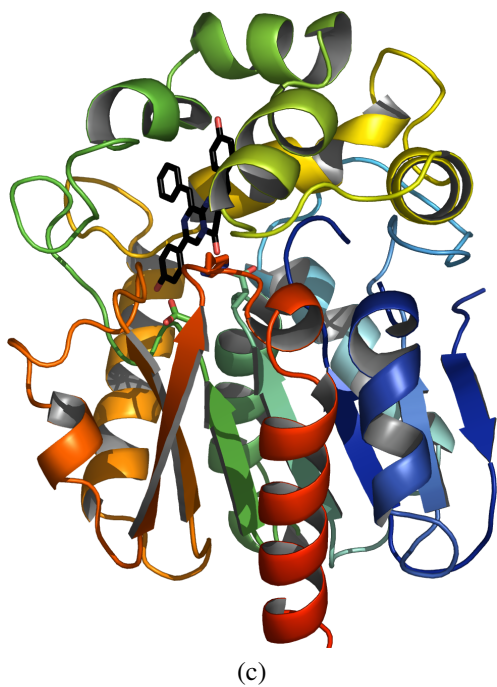
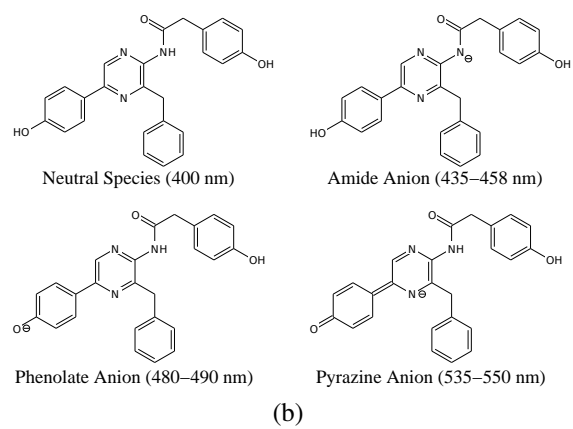
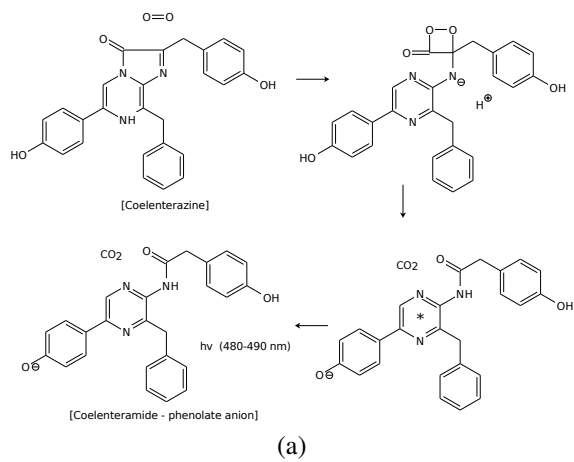
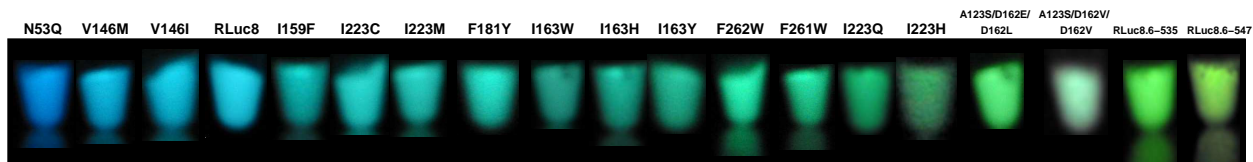
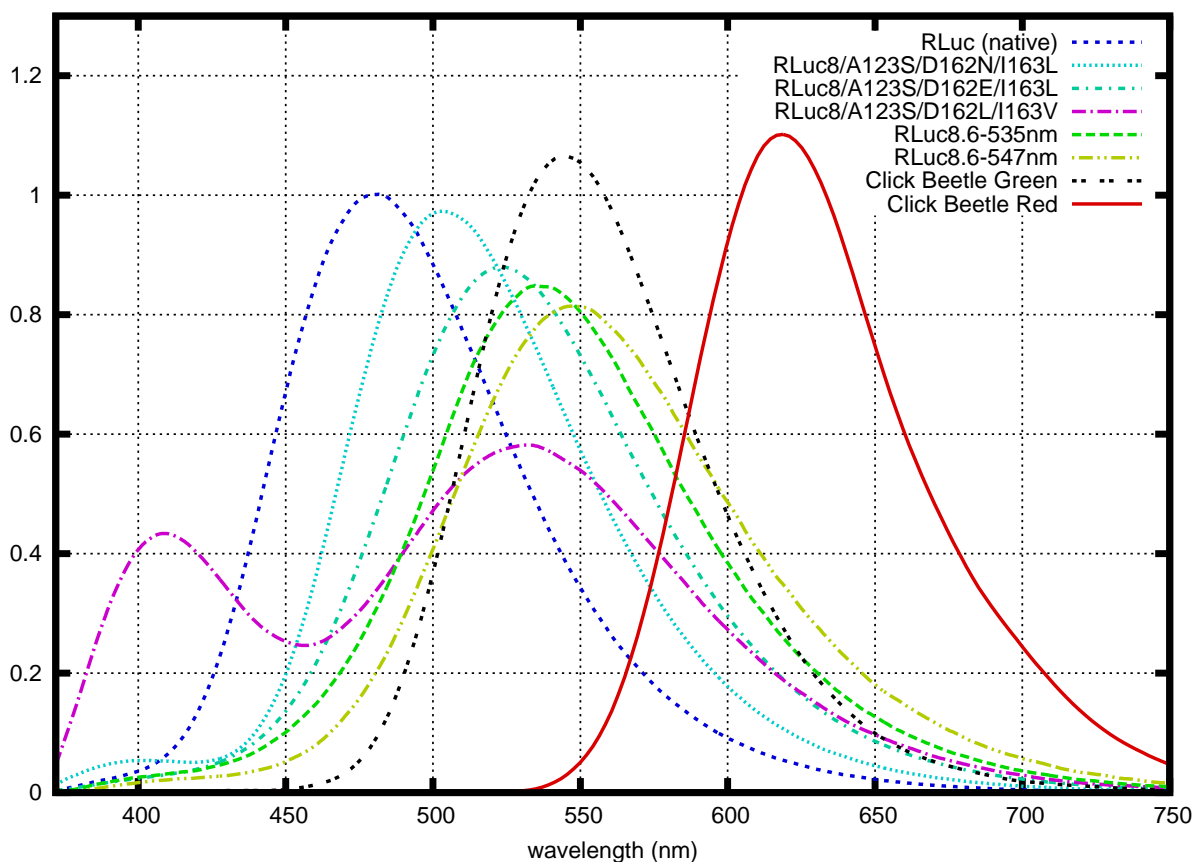


Figure 1:

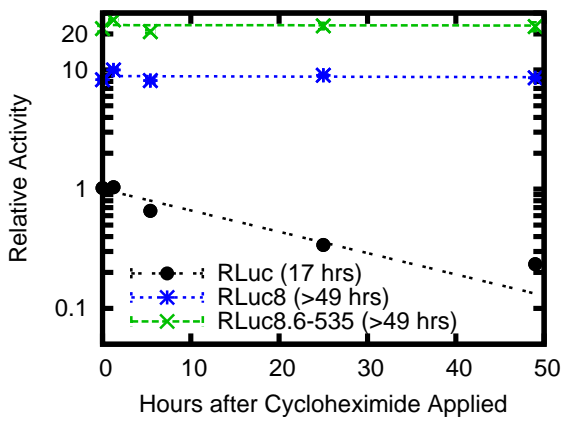


(a)

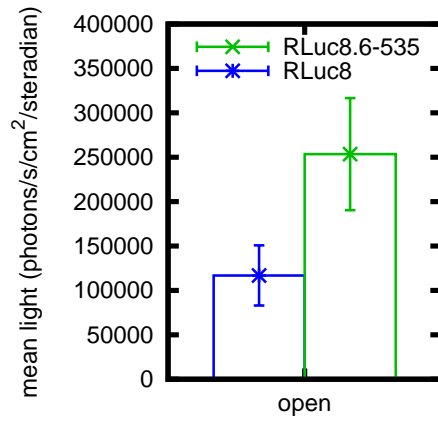


(b)

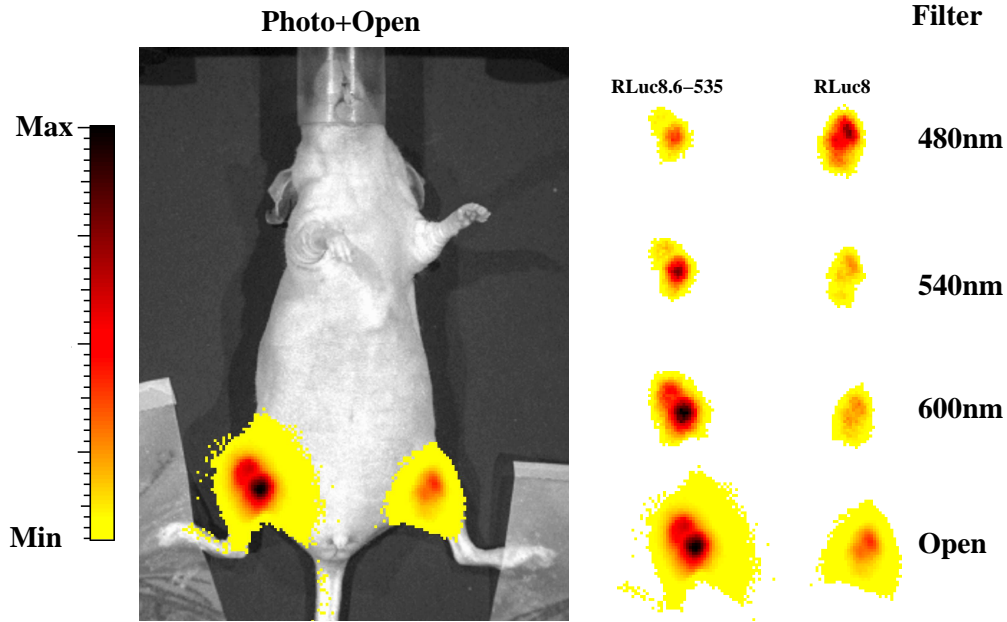
Figure 2:



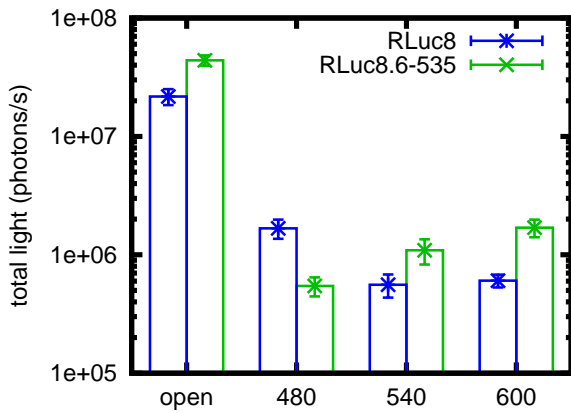
(a)



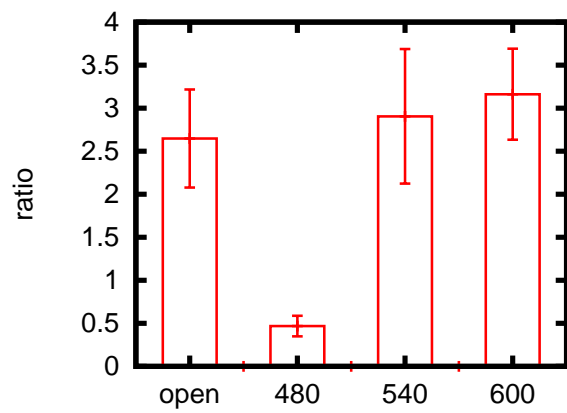
(b)



(c)



(d)



(e)

20
Figure 3:

Legends to Tables

- 1 Selected results of site-directed mutagenesis in the active pocket of RLuc8 and highlighted results from several rounds of random mutagenesis. The specific activity of RLuc in absolute terms (photons/s/mole enzyme) was 3.2×10^{22} , and all other specific activities are relative to this value. If the spectrum had a shoulder peak, it is noted above along with the ratio of the height of the shoulder peak to the main peak. FWHM - full width at half maximum. Error is standard error of the mean. 22
- 2 Effects of tissue depth on the relative light output of several *Renilla* luciferase variants. “% Transmitted” is the percent of photons that are calculated to be transmitted through the given depth of rat liver tissue. “Effective Output” is the specific activity of the enzyme multiplied by the percent of photons transmitted for the given depth, normalized to the values for RLuc. 23

	Specific Activity	Wavelength (nm)				Shoulder/ Peak Ratio	%>600 nm
		peak	mean	fwhm	shoulder		
RLuc	1.0±0.1	481	497	93			3
RLuc8	4.3±0.2	486	503	94			4
Select Active Pocket Mutations							
RLuc8/N53Q	0.10	475	491	92			3
RLuc8/V146M	1.0	481	498	94			3
RLuc8/I150H	0.64	494	514	98			6
RLuc8/I159Y	0.005	513	536	113			13
RLuc8/I163Y	0.16	502	521	103			8
RLuc8/I166Y	0.25	493	508	99			5
RLuc8/F181Y	0.08	497	515	103			6
RLuc8/I223C	3.9	503	524	103			9
RLuc8/I223H	0.09	508	527	105			9
RLuc8/F261W	0.26	504	524	98			8
RLuc8/F262W	0.75	500	521	99			7
Random Mutagenesis Results							
RLuc8/A123S	2.8	484	502	92			4
RLuc8/A123S/D162N/I163L	3.1	507	523	93	404	0.07	7
RLuc8/A123S/D162E/I163L	3.6	523	538	102			12
RLuc8/A123S/D162L/I163V	0.35	532	515	124	409	0.75	13
RLuc8/A123S/D162E/I163L/V185L	3.4	532	545	106			15
RLuc8.6-535	6.0	535	550	104			17
RLuc8.6-545	1.9	545	560	106			21
RLuc8.6-547	1.2	547	564	111			23

RLuc8.6-535 = RLuc8/A123S/D154M/E155G/D162E/I163L/V185L
RLuc8.6-545 = RLuc8/A123S/D154K/E155N/D162E/I163L/F261W
RLuc8.6-547 = RLuc8/A123S/D154A/E155G/D162E/I163V/F262W

Table 1:

	Specific Activity	Wavelength mean (nm)	% Transmitted		Effective Output	
			1 mm	5 mm	1 mm	5 mm
RLuc	1.0	497	2.8	0.025	1.0	1.0
RLuc8	4.3	503	3.1	0.029	4.7	5.0
RLuc8/A123S/D162L/I163V	0.35	515	5.7	0.17	0.71	2.4
RLuc8/A123S/D162N/I163L	3.1	523	4.2	0.065	4.7	8.1
RLuc8/A123S/D162E/I163L	3.6	538	5.8	0.13	7.4	19
RLuc8/A123S/D162E/I163L/V185L	3.4	545	6.9	0.18	8.4	25
RLuc8.6-535	6.0	550	7.4	0.20	16	48
RLuc8.6-545	1.9	560	8.7	0.26	5.9	20
RLuc8.6-547	1.2	564	9.7	0.31	4.2	15

Table 2:

Supplemental Material

Benzyl-coelenterazine (coelenterazine-*h*) was a generous gift from Dr. Bruce Bryan. Coelenterazine-*n* and coelenterazine-*cp* were from Biotium (Hayward, CA). Bisdeoxycoelenterazine (coelenterazine-*400a*, di-dehydro coelenterazine, DeepBlueC) was from Perkin Elmer (Boston, MA). The analogs were dissolved in propylene glycol and stored in small aliquots at -80°C.

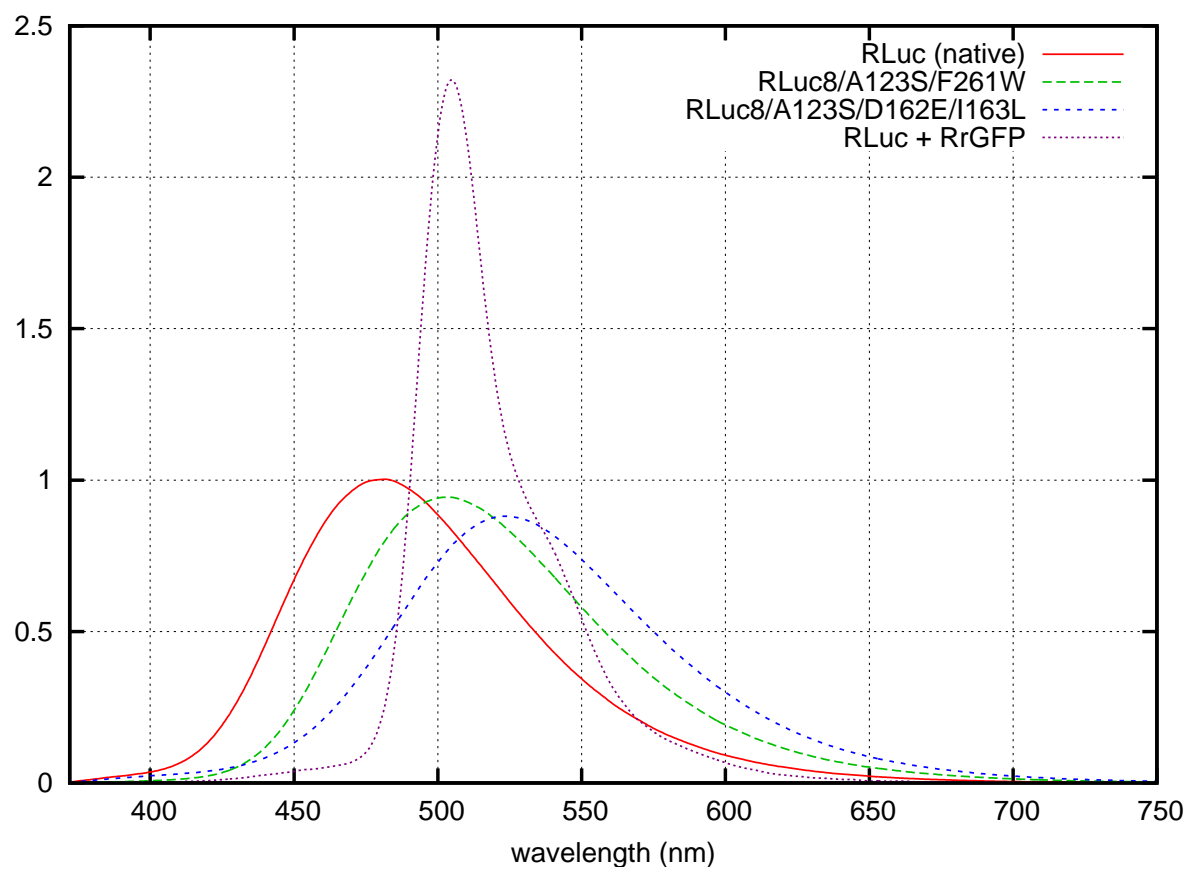
List of Supplemental Figures

- 1 Sequence of RLuc8 with residues surrounding the putative active pocket marked. The putative active pocket residues are indicated by the black bar above the sequence. RLuc8 has been aligned, using CLUSTAL W, with RLuc, the luciferase from *Renilla mulleri* (RmLuc), and two proteins of unknown function predicted from the *Strongylocentrotus purpuratus* (Purple Sea Urchin) genome (XP_787066 - GenBank Identifiers GI:72160391, XP_794218.1 - GI:72149470). Note that RLuc8 and associated variants used in this paper have an additional valine/aspartate (Sall restriction site) followed by a 6x-His tag on the C-terminus, and begin with alanine following cleavage of the pelB sequence that has replaced the initial methionine. 26
- 2 A comparison of the *Renilla reniformis* Green Fluorescent Protein (RrGFP) emission spectrum and the emission spectra of RLuc and several of its variants. The RrGFP emission spectrum was made by combining RrGFP dimer with RLuc at a 1:1 molar ratio, adding coelenterazine, and measuring the emission in the same manner as for the RLuc variants. RrGFP production and purification is described elsewhere [27]. 27
- 3 Estimated effects to the normalized emission spectra from various RLuc mutants as well as the Click Beetle luciferases after passing through either 1 mm or 5 mm of rat liver tissue. The curves were made by multiplying the normalized emission spectra by the calculated absorbance values for the different thicknesses of rat liver. This comparison assumes that all the luciferases emit an equal number of photons. The Click Beetle luciferase emission spectra are from Zhao *et al.* [6]. 28
- 4 A schematic diagram of a site-specific random mutagenesis scheme using a type II restriction enzyme. In this particular example the mutagenesis target, shown in yellow, is V185/L186. The restriction enzyme recognition sites for BpiI are shown in green. Random nucleotides are represented as follows: N=A/T/C/G, and S=C/G. For an NNS sequences, amino acids with only one codon have a 1/32 chance of being used. To have at least a 99% probability of hitting a given pair of codons, ~5000 colonies need to be screened. 29

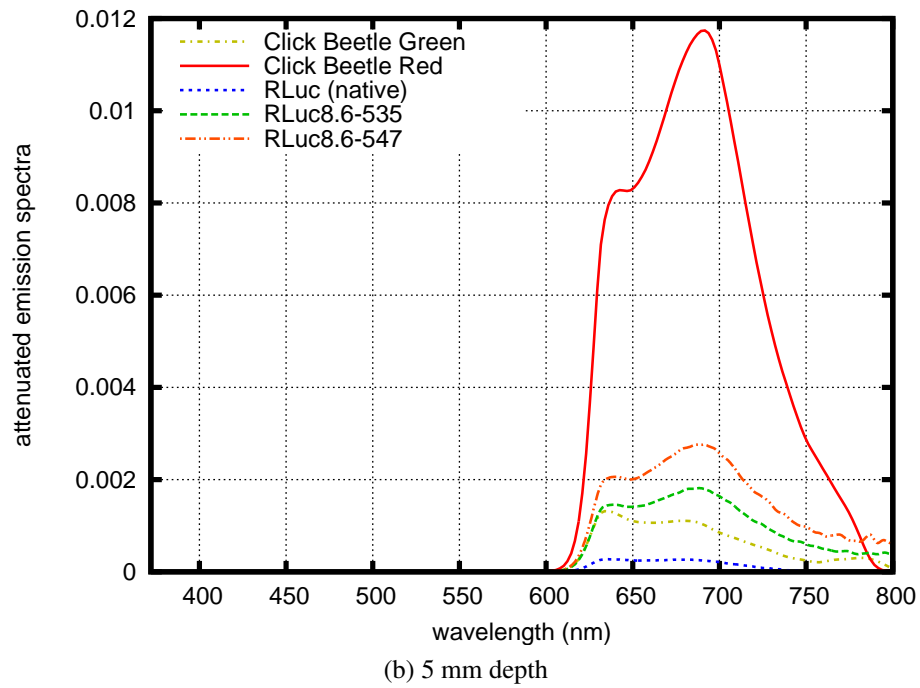
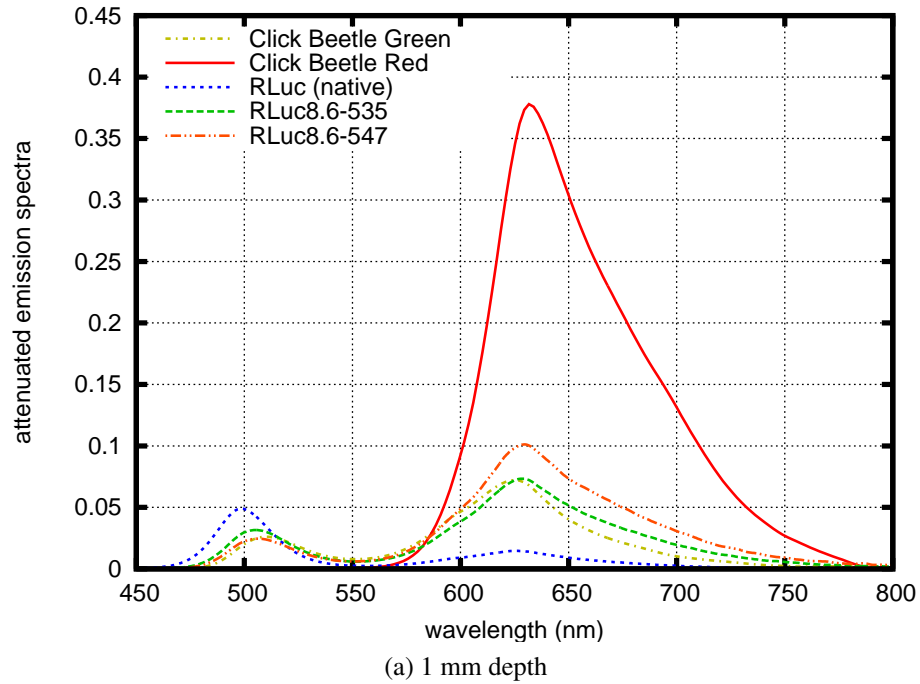
RLuc8	MA SKVYDPEQ RKRMITGPOWWARCKQMNVLDSFINYYDSE...KHAENAV	47
RLuc	MT SKVYDPEQ RKRMITGPOWWARCKQMNVLDSFINYYDSE...KHAENAV	47
RmLuc	MT SKVYDPEL RKRMITGPOWWARCKQMNVLDSFINYYDSE...KHAENAV	47
XP_787066	AA AMGSRNQ STIPLVTAD EWWGKCKKV DVLG EKMSYYDSD P QNSS SKHAV	80
XP_794218.1	...MASRNQ ATIPLVTAD EWWGKCKKV DVLG SKMSYYDSD P QN RSGKHTA	47
RLuc8	I FLHGNA TSSYLWRHVVP H IEPVARCIIPDLIGMGKSGKSGNGSYRLLDH	97
RLuc	I FLHGNA ASSYLWRHVVP H IEPVARCIIPDLIGMGKSGKSGNGSYRLLDH	97
RmLuc	I FLHGNA ASSYLWRHVVP H IEPVARCIIPDLIGMGKSGKSGNGSYRLLDH	97
XP_787066	V FLHGNP TSSYLWRNVMP QVEPTARCLAPDLIGQGRSNKLANHSYRFVDH	130
XP_794218.1	V FLHGNP TSSYLWRNVLP QVEPTARCLAPDLIGGRSDKLANASRSYRF LDH	97
RLuc8	Y KYLTAWFEL LNLPKKI IFVGHDWGA ALAFHY AYEHQDRIKAIVHMESVV	147
RLuc	Y KYLTAWFEL LNLPKKI IFVGHDWGAC LAFHY SYEHQDK IKAIVHAE SVV	147
RmLuc	Y KYLTAWFEL LNLPKKI IFVGHDWGAC LAFHY CYEHQDRIKAVVHAE SVV	147
XP_787066	Y RYLSAWFDS VNLPEKVC I VCHDWG SGLGFHW CNEHRDRIEGLIHME SVV	180
XP_794218.1	Y RYLSAWFDA LRLPEK I TVVCHDWGT ALGLHWC SEHRDRIEAIVHME GVL	147
RLuc8	D VIESWDEWPD IEEDIALIK . SEE GEKMLENN FVET V LPSKIMRKLEP	196
RLuc	D VIESWDEWPD IEEDIALIK . SEE GEKMLENN FVET M LPSKIMRKLEP	196
RmLuc	D VIESWDEWPD IEEDIALIK . SEE GEKMLENN FVET M LPSKIMRKLEP	196
XP_787066	A PVPGWDRFPD MAKDFFOYLR SEACD DLVLQKNYFTEL L LPRATIMPELRP	230
XP_794218.1	K P M T . W D I F P D S M R D I F L A L R S D A G E M I L K K N M F I E T I L P L A I K R K L R Q	196
RLuc8	E EFAAYLEPFKEKGEVRRP T LSWPREIPLVKGGKPDVVQ I VRNYNAYLRA	246
RLuc	E EFAAYLEPFKEKGEVRRP T LSWPREIPLVKGGKPDVVQ I VRNYNAYLRA	246
RmLuc	E EFAAYLEPFKEKGEVRRP T LSWPREIPLVKGGKPDVVE I VRNYNAYLRA	246
XP_787066	E EMDAYREPFKNP GEDRRP T L T W P R E I P I K G D C P D D V I A I A S S Y N A W L K E	280
XP_794218.1	E EMDAYREPFKNP GEDRRP L L T F P R Q I P I Q G E G P E T V A I A T A Y H A W I K G	246
RLuc8	S D D L P K L F I E S D P G F F S N A I V E G A K K F P N T E F V K V K G L H F S Q E D A P D E M G	296
RLuc	S D D L P K M F I E S D P G F F S N A I V E G A K K F P N T E F V K V K G L H F S Q E D A P D E M G	296
RmLuc	S H D L P K M F I E S D P G F F S N A I V E G A K K F P N T E F V K V K G L H F S Q E D A P D E M G	296
XP_787066	S A D L P K L Y I H A R P G F F S E G I K K G I A N W P N Q K T V E S E G L H F L Q E D S P I Q I G	330
XP_794218.1	T A D L P K F C I L A T P G I F S E W G T G I T K D W P N H K V V Q V E G S H F F Q E D S P I Q T G	296
RLuc8	K Y I K S F V E R V L K N E Q	311
RLuc	K Y I K S F V E R V L K N E Q	311
RmLuc	N Y I K S F V E R V L K N E Q	311
XP_787066	D H V K D F L S A L Y K . . .	342
XP_794218.1	D Y I K E F L S S V F K . . .	308

non conserved
 similar
 conserved
 all match

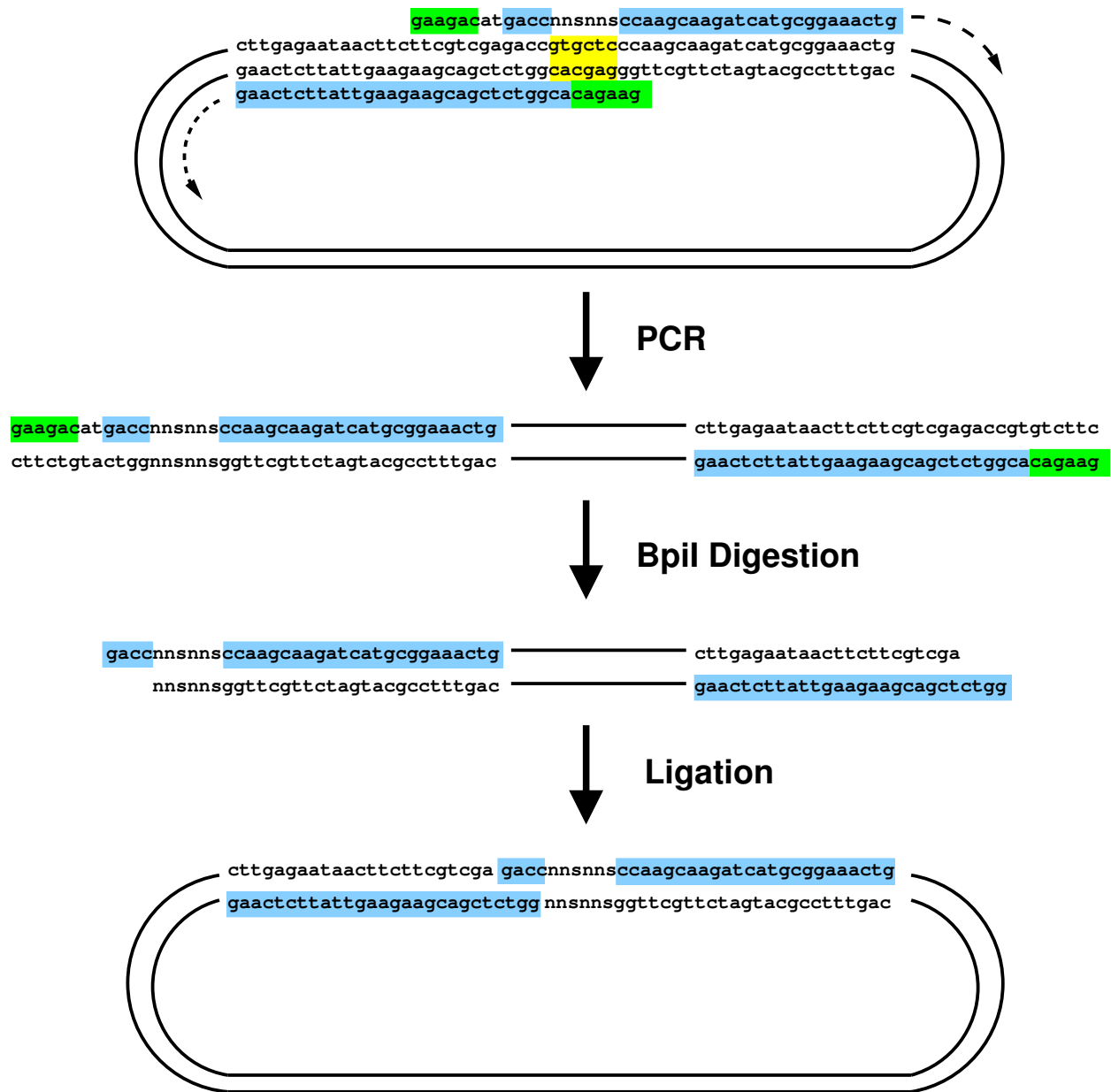
Supplemental Figure 1:



Supplemental Figure 2:



Supplemental Figure 3:



Supplemental Figure 4:

List of Supplemental Tables

- 1 Results of site-directed mutagenesis in the active pocket of RLuc8. Results for I223 are shown in Table 2. Abbreviations for substrates are *c* = coelenterazine (native substrate), *bc* = benzyl-coelenterazine, *cp* = coelenterazine-*cp*, *cn* = coelenterazine-*n*, *bdc* = bisdeoxycoelenterazine. Spectra were measured using coelenterazine. Specific activities are given as relative to that of RLuc for the given substrate, and were corrected for the luminometer's wavelength dependent sensitivity only for the substrate coelenterazine. Specific activities of RLuc in absolute terms for the different analogs are 3.2×10^{22} , 5.4×10^{22} , 1.7×10^{22} , 8.3×10^{21} , and 5.8×10^{19} photons/sec/mole enzyme for *c*, *bc*, *cp*, *cn*, and *bdc*, respectively [14]. †RLuc8/I166W showed a shoulder peak at 415 nm that was 28% of the height of the main peak at 498 nm. FWHM - full width at half maximum. ND - not determined. 32
- 2 Results of saturation mutagenesis on RLuc8 at the putative active pocket residue of I223. Substrate abbreviations are as before. Spectra were measured using coelenterazine. Specific activities are given as relative to that of RLuc for the given substrate, and were corrected for the luminometer's wavelength dependent sensitivity only for the substrate coelenterazine. FWHM - full width at half maximum. ND - not determined. 33
- 3 Results of random mutagenesis on RLuc8/F261W and RLuc8/F262W and screening of the resultant clones. Mutation locations that showed up multiple times are designated by bold text. The data for RLuc8/F261W and RLuc8/F262W is repeated from Table 1 for the purpose of comparison. ~45,000 and ~30,000 colonies were screened for the random mutagenesis on RLuc8/F261W and RLuc8/F262W, respectively. Specific activities are relative to that of RLuc. FWHM - full width at half maximum. 34
- 4 Results from site-specific random mutagenesis at the D162/I163 residues of RLuc, RLuc8/A123S, RLuc8/A123S/F261W, and RLuc8/A123S/F262W and screening of the resultant clones. If the spectrum had a shoulder peak, it is noted above along with the ratio of the height of the shoulder peak to the main peak. Clones indicates how many colonies coded for the same protein sequences (but not necessarily the same nucleotide sequence), and is an indicator for how well the search space was covered. ~8000, ~4,000, ~8,000, and ~10,000 colonies were screened from the RLuc8, RLuc8/A123S, RLuc8/A123S/F261W, and RLuc8/A123S/F262W mutagenesis reactions, respectively. The data for RLuc, RLuc8/A123S/F261W, and RLuc8/A123S/F262W is repeated from previous tables for the purpose of comparison. Specific activities are relative to that of RLuc. FWHM - full width at half maximum. 35

5	Results from site-specific random mutagenesis at V185/L186 followed by selection of the resultant clones. The templates used for mutagenesis were RLuc8 and RLuc8/A123S/D162E/I163L, and for the purposes of comparison the data for these variants is repeated from previous tables. Approximately 20,000 colonies were screened for each of the V185/L186 mutagenesis reactions. Specific activities are relative to that of RLuc. FWHM - full width at half maximum.	36
6	Results from site-specific random mutagenesis at the D154/E155 residues with selection of the resultant clones. The templates used for mutagenesis were RLuc8/A123S/D162E/I163L/V185L, RLuc8/A123S/D162E/I163L/F261W, and RLuc8/A123S/D162E/I163V/F262W. The data for these parental constructs are repeated from previous tables for the purpose of comparison. Approximately 3000-9000 colonies were screened from each template. Specific activities are relative to that of RLuc. FWHM - full width at half maximum.	37
7	Specific activities and emission spectra data for RLuc, RLuc8, and several variants measured with various coelenterazine analogs. Abbreviations for substrates are as before. Specific activities are given as relative to that of RLuc for the given substrate, and were corrected for the luminometer's wavelength dependent sensitivity for all substrates. Absolute values for the specific activity of RLuc are given in a previous table legend. Some data has been repeated here from previous tables for the purpose of comparison. RLuc8/A123S/D162L/I163V showed a shoulder peak at 409, 412, 407, and 411 nm with a height ratio to the main peak of 0.75, 0.83, 0.75, and 0.60 for <i>c</i> , <i>bc</i> , <i>cp</i> , and <i>cn</i> , respectively. ND - not determined.	38

	Specific Activity (relative to RLuc)					Wavelength (nm)			%>600 nm
	c	bc	cp	cn	bdc	peak	mean	fwhm	
RLuc	1.0±0.1	1.0	1.0	1.0	1.0	481	497	93	3
RLuc8	4.3±0.2	3.0	5.8	8.8	59	486	503	94	4
Active Pocket Mutations									
RLuc8/N53D	0.002	0.004	0.002	0.001	0.01			ND	
RLuc8/N53Q	0.10	0.16	0.52	0.04	0.31	475	491	92	3
RLuc8/N53S	0.001	0.002	0.003	0.005	0.03			ND	
RLuc8/W121F	0.05	0.02	0.02	0.03	0.15	478	496	94	3
RLuc8/W121H	0.003	0.002	0.004	0.01	0.02			ND	
RLuc8/W121Y	0.003	0.007	0.01	0.01	0.01			ND	
RLuc8/V146I	1.1	1.1	0.60	0.50	21	484	502	95	4
RLuc8/V146M	1.0	0.66	0.51	0.47	0.43	481	498	94	3
RLuc8/V146W	0.000	0.000	0.000	0.000	0.000			ND	
RLuc8/I150F	0.51	0.56	0.50	1.0	5.3	485	504	95	4
RLuc8/I150H	0.64	0.30	0.23	3.1	8.1	494	514	98	6
RLuc8/I150M	3.2	2.0	3.4	2.4	24	488	508	95	5
RLuc8/I150W	0.94	0.65	0.62	1.3	8.2	485	503	94	4
RLuc8/I150Y	0.02	0.01	0.02	0.32	0.15	487	506	97	4
RLuc8/W153F	4.9	3.1	4.9	7.9	104	484	502	95	4
RLuc8/W153Y	1.2	0.75	1.1	2.1	15	485	503	96	4
RLuc8/W156F	3.9	2.7	7.2	12	81	486	504	93	4
RLuc8/W156H	0.51	0.53	0.58	2.5	1.2	490	510	96	5
RLuc8/W156Y	3.0	2.6	5.2	9.0	91	483	501	94	4
RLuc8/I159F	0.66	0.47	0.62	1.9	1.4	491	510	101	5
RLuc8/I159H	0.05	0.05	0.03	0.14	0.53	506	526	108	10
RLuc8/I159W	0.13	0.14	0.09	0.48	0.28	490	508	104	6
RLuc8/I159Y	0.005	0.003	0.02	0.08	1.1	513	536	113	13
RLuc8/I163F	0.57	0.80	0.39	0.61	7.6	483	502	95	4
RLuc8/I163H	0.16	0.21	0.12	0.19	6.1	499	519	102	7
RLuc8/I163W	0.19	0.31	0.18	0.31	2.1	498	517	103	7
RLuc8/I163Y	0.16	0.19	0.12	0.17	1.2	502	521	103	8
RLuc8/I166F	1.3	1.2	1.1	1.8	11	483	501	96	4
RLuc8/I166H	0.04	0.08	0.03	0.05	0.52	483	502	100	4
RLuc8/I166L	4.4	2.4	5.3	9.5	55	486	506	92	4
RLuc8/I166W	0.004	0.01	0.003	0.01	0.20	498 [†]	508	110	7
RLuc8/I166Y	0.25	0.39	0.18	0.37	2.5	493	508	99	5
RLuc8/F180I	0.63	0.65	0.62	0.70	8.7	486	504	101	5
RLuc8/F180W	4.0	2.4	3.3	4.6	45	485	502	93	4
RLuc8/F180Y	3.0	2.2	2.6	3.4	52	484	499	105	4
RLuc8/F181W	0.07	0.05	0.05	0.13	4.8	479	494	95	3
RLuc8/F181Y	0.08	0.13	0.04	0.07	1.2	497	515	103	6
RLuc8/K189E	4.4	2.6	3.8	6.7	61	484	501	95	4
RLuc8/K189H	3.6	2.0	1.8	6.1	44	485	502	94	4
RLuc8/K189I	1.1	1.0	4.4	1.9	19	484	500	96	4
RLuc8/K189R	0.70	0.86	0.58	0.45	1.1	484	502	93	4
RLuc8/P220H	0.003	0.003	0.003	0.01	0.05			ND	
RLuc8/P224H	0.08	0.03	0.07	0.004	0.29	484	500	95	4
RLuc8/F261W	0.26	0.49	0.49	0.03	0.76	504	524	98	8
RLuc8/F261Y	0.07	0.93	0.53	0.01	16	487	506	97	4
RLuc8/F261W/F262W	0.000	0.000	0.00	0.002	0.003	512	531	115	11
RLuc8/F262W	0.75	0.25	0.29	0.09	0.02	500	521	99	7
RLuc8/F262Y	0.01	0.01	0.01	0.001	0.04	511	532	104	10
RLuc8/F286W	0.08	0.11	0.07	0.04	0.24	481	499	92	3
RLuc8/F286Y	0.07	0.08	0.23	0.05	0.24	482	501	93	4

Supplemental Table 1:

	Specific Activity (relative to RLuc)					Wavelength (nm)			%>600 nm
	c	bc	cp	cn	bdc	peak	mean	fwhm	
RLuc	1.0±0.1	1.0	1.0	1.0	1.0	481	497	93	3
RLuc8	4.3±0.2	3.0	5.8	8.8	59	486	503	94	4
I223 Mutations									
RLuc8/I223A	0.68	0.37	0.94	0.51	2.0			ND	
RLuc8/I223C	3.9	2.2	8.1	4.8	12	503	524	103	9
RLuc8/I223D	0.01	0.01	0.01	0.06	0.10	503	524	106	9
RLuc8/I223E	0.01	0.01	0.01	0.11	0.21	497	517	104	7
RLuc8/I223F	2.7	2.1	1.8	2.5	10	486	505	92	4
RLuc8/I223G	0.17	0.08	0.14	0.40	1.3	498	518	105	7
RLuc8/I223H	0.09	0.07	0.12	0.56	1.9	508	527	105	9
RLuc8/I223K	0.002	0.002	0.001	0.003	0.26	491	509	97	5
RLuc8/I223L	1.3	1.8	1.2	1.4	16	483	502	95	4
RLuc8/I223M	0.24	0.46	0.31	0.80	14	501	521	98	7
RLuc8/I223N	0.39	0.40	0.43	0.62	1.7	505	527	102	9
RLuc8/I223P	0.01	0.01	0.01	0.03	0.13	486	505	96	5
RLuc8/I223Q	0.08	0.08	0.08	0.40	2.3	505	527	102	9
RLuc8/I223R	0.004	0.003	0.003	0.01	0.24	505	528	108	10
RLuc8/I223S	0.73	0.54	0.59	0.85	1.7	499	517	104	7
RLuc8/I223T	0.52	0.43	0.40	0.58	0.54	499	517	102	7
RLuc8/I223V	2.8	2.1	3.1	3.3	31	490	509	97	5
RLuc8/I223W	0.003	0.004	0.01	0.02	0.01	484	508	104	7
RLuc8/I223Y	0.02	0.02	0.02	0.04	0.07	486	505	97	4

Supplemental Table 2:

F261W Mutants	Specific Activity	Wavelength (nm)			%>600 nm
		peak	mean	fwhm	
RLuc8/F261W	0.26	505	524	98	8
RLuc8/R11P/F261W/V267I	0.33	501	522	99	7
RLuc8/A22P/ D162N /F261W	0.16	526	547	97	13
RLuc8/V63I/ L94F /F261W/F278I	0.47	501	522	98	7
RLuc8/R93L/ D162E /F261W	0.09	535	551	112	17
RLuc8/ L94F /F261W	0.19	501	521	97	7
RLuc8/K113R/ E155K /F261W	0.70	503	523	98	7
RLuc8/ A123S /F261W	0.63	504	523	98	7
RLuc8/M143T/F261W	0.34	503	523	98	7
RLuc8/ D162N /F261W/S188N	0.08	525	544	97	13
RLuc8/A164T/D248E/F261W/K297N	0.16	502	521	98	7
RLuc8/F261W/N264S	0.35	503	523	99	7
RLuc8/F261W/K271R	0.18	505	526	99	8
F262W Mutants					
RLuc8/F262W	0.75	500	521	99	7
RLuc8/Q26K/ E155K /F262W	0.94	500	521	99	7
RLuc8/P65H/A130T/F262W	0.15	501	522	99	8
RLuc8/F105V/E151K/ D162E /F262W	0.12	535	551	119	18
RLuc8/ A123S /F262W	0.63	499	519	98	7
RLuc8/ E155G /E183D/F262W	1.1	501	522	98	7
RLuc8/ E155K /E169D/F262W	0.75	501	521	98	7
RLuc8/K167M/K173N/F262W	0.68	498	519	98	7
RLuc8/V234I/F262W/ G269R	1.1	501	523	99	8
RLuc8/F262W/ G269E	0.71	500	520	98	7
RLuc8/F262W/ G269R	1.7	502	523	100	8
RLuc8/F262W/M295V	0.59	499	520	98	7

Supplemental Table 3:

RLuc8 Mutants	Specific Activity	Wavelength (nm)				Shoulder/ Peak Ratio	%>600 nm	Clones
		peak	mean	fwhm	shoulder			
RLuc8	4.3	486	503	94			4	
RLuc8/D162E	2.1	522	537	108			12	1
RLuc8/D162E/I163M	1.7	519	530	108			10	1
RLuc8/D162E/I163T	0.14	539	547	125			19	1
RLuc8/D162N	2.7	510	526	96	408	0.05	8	2
RLuc8/D162N/I163V	2.2	516	531	103	408	0.08	10	6
RLuc8/D162P/I163L	0.35	525	515	103	406	0.50	10	1
RLuc8/D162S/I163V	4.7	485	504	92			4	1
RLuc8/A123S Mutants								
RLuc8/A123S	2.8	484	502	92			4	
RLuc8/A123S/D162C/I163V	1.4	520	539	94			11	1
RLuc8/A123S/D162E	2.3	522	536	107			12	2
RLuc8/A123S/D162E/I163L	3.6	523	538	102			12	2
RLuc8/A123S/D162L/I163V	0.35	532	515	124	409	0.75	13	1
RLuc8/A123S/D162N	2.6	509	526	96	407	0.05	8	1
RLuc8/A123S/D162N/I163L	3.1	507	523	93	404	0.07	7	2
RLuc8/A123S/D162N/I163S	0.29	523	535	110	407	0.18	13	2
RLuc8/A123S/D162T/I163C	0.12	527	514	119	409	0.69	12	1
RLuc8/A123S/F261W Mutants								
RLuc8/A123S/F261W	0.62	504	523	98			7	
RLuc8/A123S/D162T/F261W	0.39	526	547	102			14	1
RLuc8/A123S/D162E/F261W	0.36	533	547	116			16	1
RLuc8/A123S/D162E/I163L/F261W	0.20	538	553	107			17	
RLuc8/A123S/D162N/I163M/F261W	0.44	520	539	95			11	3
RLuc8/A123S/D162N/I163V/F261W	0.36	531	551	102			16	3
RLuc8/A123S/F262W Mutants								
RLuc8/A123S/F262W	0.63	499	519	98			7	
RLuc8/A123S/D162E/I163V/F262W	0.12	541	558	113			21	1
RLuc8/A123S/D162N/F262W	0.37	527	544	100			13	1

Supplemental Table 4:

RLuc8 Mutants	Specific Activity	Wavelength (nm)			%>600 nm
		peak	mean	fwhm	
RLuc8	4.3±0.2	486	503	94	4
RLuc8/V185L	3.3	485	504	95	4
RLuc8/V185Q	4.5	482	500	93	3
RLuc8/A123S/D162E/I163L Mutants					
RLuc8/A123S/D162E/I163L	3.6	523	538	102	12
RLuc8/A123S/D162E/I163L/V185L	3.4	532	545	106	15
RLuc8/A123S/D162E/I163L/V185L/L186F	1.1	530	541	110	14

Supplemental Table 5:

RLuc8/A123S/D162E/I163L/V185L Mutants	Specific Activity	Wavelength (nm)			% > 600 nm
		peak	mean	fwhm	
RLuc8/A123S/D162E/I163L/V185L	3.4	532	545	106	15
RLuc8/A123S/D154M/E155G/D162E/I163L/V185L	6.0	535	550	104	17
RLuc8/A123S/D154R/E155T/D162E/I163L/V185L	4.6	531	546	104	15
RLuc8/A123S/E155G/D162E/I163L/V185L	5.4	532	545	104	15
RLuc8/A123S/D162E/I163L/F261W Mutants					
RLuc8/A123S/D162E/I163L/F261W	0.22	538	553	107	17
RLuc8/A123S/D154K/E155N/D162E/I163L/F261W	1.9	545	560	106	21
RLuc8/A123S/D154R/E155G/D162E/I163L/F261W	0.70	537	554	106	18
RLuc8/A123S/E155G/D162E/I163L/F261W	1.2	537	554	107	17
RLuc8/A123S/E155K/D162E/I163L/F261W	0.83	541	556	107	18
RLuc8/A123S/D162E/I163V/F262W Mutants					
RLuc8/A123S/D162E/I163V/F262W	0.12	541	558	113	21
RLuc8/A123S/D154A/E155G/D162E/I163V/F262W	1.2	547	564	111	23
RLuc8/A123S/D154T/E155G/D162E/I163V/F262W	1.1	544	560	112	21
RLuc8/A123S/D154V/E155G/D162E/I163V/F262W	1.7	543	560	112	21
RLuc8/A123S/E155G/D162E/I163V/F262W	1.6	543	560	111	21

Supplemental Table 6:

	Specific Activity					Peak Wavelength (nm)					Mean Wavelength (nm)				
	<i>c</i>	<i>bc</i>	<i>cp</i>	<i>cn</i>	<i>bdc</i>	<i>c</i>	<i>bc</i>	<i>cp</i>	<i>cn</i>	<i>bdc</i>	<i>c</i>	<i>bc</i>	<i>cp</i>	<i>cn</i>	<i>bdc</i>
RLuc	1.0	1.0	1.0	1.0	1.0	481	483	477	487	405	497	499	493	505	433
RLuc8	4.3	3.0	5.8	8.8	59	486	487	477	486	402	503	504	494	504	423
RLuc8/A123S/D162N/I163L	3.1	1.6	3.1	2.4	8.7	507	512	501	509	397	523	527	516	526	430
RLuc8/A123S/D162E/I163L	3.6	2.6	4.2	2.9	44	523	526	515	526	396	538	540	529	540	422
RLuc8/A123S/D162L/I163V	0.35	0.20	0.28	0.14	12	532	534	507	522	396	515	515	520	517	425
RLuc8/A123S/D162E/I163L/V185L	3.4	1.9	1.1	2.2	15	532	533	523	533	399	545	547	536	546	436
RLuc8.6-535	6.0	2.8	4.4	5.6	29	535	532	525	534	397	550	545	538	548	424
RLuc8.6-545	1.9	1.1	3.1	0.88	6.6	545	541	529	539	405	560	556	543	554	446
RLuc8.6-547	1.2	0.23	0.35	1.4	0.44	547	547	532	542	ND	564	561	547	559	ND

Supplemental Table 7: